

A high-speed avalanche photodiode*

Li Bin(李彬), Yang Xiaohong(杨晓红), Yin Weihong(尹伟红), Lü Qianqian(吕倩倩),
Cui Rong(崔荣), and Han Qin(韩勤)[†]

State Key Laboratory of Integrated Optoelectronics, Institute of Semiconductors, Chinese Academy of Sciences,
Beijing 100083, China

Abstract: High-speed avalanche photodiodes are widely used in optical communication systems. Nowadays, separate absorption charge and multiplication structure is widely adopted. In this article, a structure with higher speed than separate absorption charge and multiplication structure is reported. Besides the traditional absorption layer, charge layer and multiplication layer, this structure introduces an additional charge layer and transit layer and thus can be referred to as separate absorption, charge, multiplication, charge and transit structure. The introduction of the new charge layer and transit layer brings additional freedom in device structure design. The benefit of this structure is that the carrier transit time and device capacitance can be reduced independently, thus the 3 dB bandwidth could be improved by more than 50% in contrast to the separate absorption charge and multiplication structure with the same size.

Key words: avalanche photodiodes; photodetector; high speed

DOI: 10.1088/1674-4926/35/7/074009

PACC: 8160C; 7340L

1. Introduction

In past decades, avalanche photodiodes (APD) have been widely used in commerce, military and scientific research. High speed APD Operating at a wavelength of 1.55 μm is crucial for high bit-rate long-haul optical communication systems. The increasing demand of high-speed receivers for optical communication systems promotes the structure development of APD. APD used in optical communication generally adopts separate absorption charge and multiplication (SACM) structure^[1]. To obtain higher speed, a lot of work has been done. Lenox *et al.*^[2] used resonant cavity structure to reduce carrier transit time and two space layers to reduce device capacitance, a unity-gain bandwidth of 24 GHz and a gain-bandwidth product of 290 GHz was achieved. Li *et al.*^[3] used undepleted absorber to reduce carrier transit time and a space layer to reduce device capacitance; a low-gain bandwidth of 20 GHz and a gain-bandwidth product of 160 GHz were achieved. To reduce device capacitance and obtain higher speed for large size devices, a transport layer was adopted^[4]. In their waveguide structure reported^[5], Kinsey *et al.* used quite thick charge layer and grading layer (280 nm) to adjust carrier transit time and device capacitance; a low-gain bandwidth of 28 GHz and a gain-bandwidth product of 320 GHz were achieved. Two undoped InGaAsP layers were adopted in an evanescently-coupled avalanche photodiode^[6] to play the same role and achieved a low-gain bandwidth of 31.5 GHz and a gain-bandwidth product of 150 GHz.

2. Research

In this article, a novel APD which has higher speed than

SACM APD is proposed. Its basic structure is shown in Fig. 1. Compared with the SACM structure, this structure has an additional charge layer and transit layer, thus it can be referred to as separate absorption, charge, multiplication, charge and transit (SACMCT) structure. The introduction of the new charge layer and transit layer brings new degrees of freedom in device design: carrier transit time can be reduced while device capacitance stays unchanged or device capacitance be reduced while carrier transit time stays unchanged, or both of them can be reduced simultaneously. Thus higher speed can be achieved.

The speed of an APD is mainly determined by three factors: carrier transit time, device capacitance-resistance time and avalanche build up time.

In APD, light is absorbed in the absorption layer and trans-

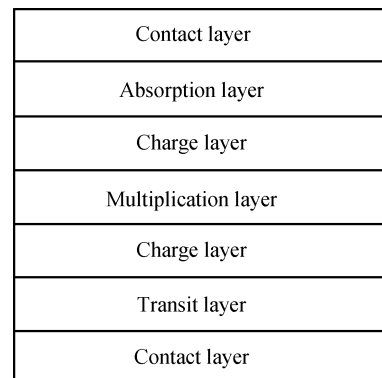


Fig. 1. Schematic diagram of separate absorption charge multiplication charge and transit structure.

* Project supported by the National Natural Science Foundation of China (Nos. 61176053, 61274069), the National Key Basic Research and Development Program of China (No. 2012CB933503), and the National High Technology Research and Development Program of China (Nos. 2012AA012202, 2013AA031401).

[†] Corresponding author. Email: hanqin@semi.ac.cn

Received 27 November 2013, revised manuscript received 8 January 2014

© 2014 Chinese Institute of Electronics

formed into electron–hole pairs. A kind of carrier drifts out of the absorption layer and reaches the contact layer while the other kind of carrier passes the charge layer and enters the multiplication layer. Take electrons entering the multiplication layer for example: electrons enter the multiplication layer, initiate avalanche multiplication and produce secondary electron–hole pairs. Secondary electron–hole pairs drift out of the multiplication layer and reach the contact layers. Device carrier transit time is thus composed of two parts: the time electrons enter the multiplication layer from the absorption layer and the secondary carrier transit time which is the time secondary carrier pairs drift from the multiplication layer to the contact layers. The latter is determined by the longer transit time of secondary electrons and holes. In ordinary SACM APD, secondary electrons drift out of the multiplication layer and reach the contact layer directly while secondary holes drift through the charge layer, absorption layer and reach the contact layer. Thus the secondary carrier transit time is the transit time of secondary holes. As to SACMCT APD, secondary electrons drift through the new charge layer and transit layer and reach the contact layer while secondary holes drift through the charge layer, absorption layer and reach the contact layer. Under the condition that secondary electron transit time is shorter than secondary hole transit time, the secondary carrier transit time is still the transit time of secondary holes. Thus carrier transit time is unchanged in the case where the thickness of the layers that originally exist is unchanged. But because of the introduction of the new charge layer and transit layer, the depletion region thickness of the device under operation increases and device capacitance decreases. Reducing the thickness of the layers that originally exist reduces the carrier transit time, but the total depletion region thickness of the new structure can still be equal to or higher than the SACM structure, i.e., the device capacitance is unchanged or reduced. Thus high-speed performance is improved.

Take the structure reported in Ref. [2] (shown in Fig. 2 and referred to as SACM below when the thickness of InAlAs space layer A is 50 nm, the thickness of InAlAs charge layer B is 150 nm, the thickness of InAlAs charge layer C is 0, and the thickness of InAlAs transit layer D is 0) for example to verify the advantage of the SACMCT structure in each of the three cases discussed above.

The 3 dB bandwidth of the device is expressed as:

$$f = \frac{1}{2\pi \sqrt{(RC)^2 + 0.36(\tau_{av} + \tau_{tr})^2}}, \quad (1)$$

where R is the series resistance which can be assumed to be 70Ω ^[7], C is the device capacitance, τ_{tr} is the carrier transit time and τ_{av} is the avalanche build up time. When electrons inject into the multiplication layer, the avalanche build up time can be expressed as:

$$\tau_{av} = Gk \frac{d_m}{v_e} + \frac{d_m}{v_h}, \quad (2)$$

where G is the avalanche multiplication gain, k is electron and hole ionization ratio, d_m is the multiplication layer thickness, v_e , v_h are electron and hole velocity: $v_e = 8 \times 10^6$ cm/s, $v_h = 6 \times 10^6$ cm/s^[7].

The value of k is reported to be 0.2^[8], 0.18^[2] and 0.1^[9] when the multiplication layer is 200 nm InAlAs. Therefore

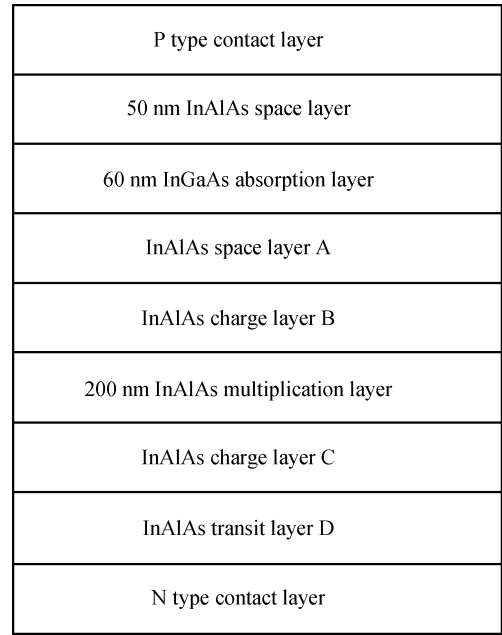


Fig. 2. Schematic diagram of the structures calculated.

the value of 0.18 is taken in the calculation below and the avalanche build up time is:

$$\begin{aligned} \tau_{av} &= 0.18G \frac{200 \text{ nm}}{8 \times 10^6 \text{ cm/s}} + \frac{200 \text{ nm}}{6 \times 10^6 \text{ cm/s}} \\ &= (4.5 \times 10^{-13} \times G + 3.3 \times 10^{-12}) \text{ s}. \end{aligned} \quad (3)$$

Figure 2 is the schematic diagram of the structures calculated. Besides the SACM structure, three devices with different parameters (referred to as SACMCT1, SACMCT2, and SACMCT3 below) were calculated. For SACMCT1, the thickness of InAlAs space layer A is 0, the thickness of InAlAs charge layer B is 50 nm, the thickness of InAlAs charge layer C is 50 nm, and the thickness of InAlAs transit layer D is 150 nm; for SACMCT2, the thickness of A, B, C, D are 50, 50, 50 and 230 nm respectively; for SACMCT3, the thickness of A, B, C, D are 150, 50, 50 and 360 nm respectively.

Assume that the thickness of the depleted P type contact layer can be ignored and the depleted N type contact layer is 50 nm for the SACM structure shown in Fig. 2 when the device is under operation. Compared to the SACM structure, the thickness of the SACMCT charge layer above the multiplication layer is reduced to 1/3 and the doping concentration is tripled, and thus the field control effect is maintained. The doping concentration of the new 50 nm charge layer equals the N type contact layer, therefore, the thickness of the depleted N type contact layer can be ignored for the SACMCT structures. Thus the depletion region thickness is 560 nm for SACM and SACMCT1, 690 nm for SACMCT2 and 920 nm for SACMCT3.

The capacitance of SACM and SACMCT1 is:

$$C = \frac{1}{\frac{d_1}{\epsilon_1 s} + \frac{d_2}{\epsilon_2 s}} = 6.31 \times 10^{-16} r^2 \text{ F}. \quad (4)$$

The capacitance of SACMCT2 is:

$$C^* = \frac{1}{\frac{d_1}{\varepsilon_1 s} + \frac{d_3}{\varepsilon_2 s}} = 5.12 \times 10^{-16} r^2 \text{ F.} \quad (5)$$

The capacitance of SACMCT3 is:

$$C^{**} = \frac{1}{\frac{d_1}{\varepsilon_1 s} + \frac{d_4}{\varepsilon_2 s}} = 3.83 \times 10^{-16} r^2 \text{ F,} \quad (6)$$

where ε_1 is the dielectric constant, d_1 is the thickness of the absorption layer, ε_2 is the dielectric constant of the InAlAs layers, d_2, d_3, d_4 are the total thickness of the depleted InAlAs layers, s is device area, and r is device radius in microns.

The carrier transit time of the SACM structure is:

$$\begin{aligned} \tau_{tr1} &= \frac{(60 + 50 + 150) \text{ nm}}{8 \times 10^6 \text{ cm/s}} + \frac{(60 + 50 + 150 + 50) \text{ nm}}{6 \times 10^6 \text{ cm/s}} \\ &= 8.42 \times 10^{-12} \text{ s.} \end{aligned} \quad (7)$$

The 3 dB bandwidth of the SACM structure can be expressed as:

$$\begin{aligned} f_1 &= 0.159 \text{ Hz} \times \left[(4.42r^2 \times 10^{-14})^2 \right. \\ &\quad \left. + 0.36(1.17 \times 10^{-11} + G \times 4.5 \times 10^{-13})^2 \right]^{-1/2}. \end{aligned} \quad (8)$$

In SACMCT1, the transit time of secondary holes is:

$$\tau_{h2} = \frac{(50 + 60 + 50) \text{ nm}}{6 \times 10^6 \text{ cm/s}} = 2.67 \times 10^{-12} \text{ s.} \quad (9)$$

The transit time of secondary electrons is:

$$\tau_{e2} = \frac{(50 + 150) \text{ nm}}{8 \times 10^6 \text{ cm/s}} = 2.5 \times 10^{-12} \text{ s.} \quad (10)$$

Thus the secondary carrier transit time is determined by the transit time of secondary holes. The total transit time is:

$$\tau_{tr2} = \frac{(60 + 50) \text{ nm}}{8 \times 10^6 \text{ cm/s}} + \frac{(60 + 50 + 50) \text{ nm}}{6 \times 10^6 \text{ cm/s}} = 4.04 \times 10^{-12} \text{ s.} \quad (11)$$

Thus SACMCT1 can reduce the carrier transit time while keeping the capacitance unchanged compared with the SACM structure.

The 3 dB bandwidth of SACMCT1 can be expressed as:

$$\begin{aligned} f_2 &= 0.159 \text{ Hz} \times \left[(4.42r^2 \times 10^{-14})^2 \right. \\ &\quad \left. + 0.36(7.34 \times 10^{-12} + G \times 4.5 \times 10^{-13})^2 \right]^{-1/2}. \end{aligned} \quad (12)$$

In SACMCT2, the transit time of secondary holes is:

$$\tau_{h3} = \frac{(50 + 60 + 50 + 50) \text{ nm}}{6 \times 10^6 \text{ cm/s}} = 3.5 \times 10^{-12} \text{ s.} \quad (13)$$

The transit time of secondary electrons is:

$$\tau_{e3} = \frac{(50 + 230) \text{ nm}}{8 \times 10^6 \text{ cm/s}} = 3.5 \times 10^{-12} \text{ s.} \quad (14)$$

The transit time of secondary holes and secondary electrons are equal, the total transit time is:

$$\begin{aligned} \tau_{tr3} &= \frac{(60 + 50 + 50) \text{ nm}}{8 \times 10^6 \text{ cm/s}} + \frac{(50 + 60 + 50 + 50) \text{ nm}}{6 \times 10^6 \text{ cm/s}} \\ &= 5.5 \times 10^{-12} \text{ s.} \end{aligned} \quad (15)$$

Thus SACMCT2 can reduce both carrier transit time and device capacitance compared with the SACM structure.

The 3 dB bandwidth of SACMCT2 can be expressed as:

$$\begin{aligned} f_3 &= 0.159 \text{ Hz} \times \left[(3.58r^2 \times 10^{-14})^2 \right. \\ &\quad \left. + 0.36(8.8 \times 10^{-12} + G \times 4.5 \times 10^{-13})^2 \right]^{-1/2}. \end{aligned} \quad (16)$$

In SACMCT3, the transit time of secondary holes is:

$$\tau_{h4} = \frac{(50 + 60 + 150 + 50) \text{ nm}}{6 \times 10^6 \text{ cm/s}} = 5.16 \times 10^{-12} \text{ s.} \quad (17)$$

The transit time of secondary electrons is:

$$\tau_{e4} = \frac{(50 + 360) \text{ nm}}{8 \times 10^6 \text{ cm/s}} = 5.13 \times 10^{-12} \text{ s.} \quad (18)$$

The total transit time is:

$$\begin{aligned} \tau_{tr4} &= \frac{(60 + 150 + 50) \text{ nm}}{8 \times 10^6 \text{ cm/s}} + \frac{(50 + 60 + 150 + 50) \text{ nm}}{6 \times 10^6 \text{ cm/s}} \\ &= 8.42 \times 10^{-12} \text{ s.} \end{aligned} \quad (19)$$

Thus SACMCT3 can reduce the capacitance while keeping the carrier transit time unchanged compared with the SACM structure.

The 3 dB bandwidth of SACMCT3 is:

$$\begin{aligned} f_4 &= 0.159 \text{ Hz} \times \left[(2.68r^2 \times 10^{-14})^2 \right. \\ &\quad \left. + 0.36(1.17 \times 10^{-11} + G \times 4.5 \times 10^{-13})^2 \right]^{-1/2}. \end{aligned} \quad (20)$$

Figure 3 is the calculated 3 dB bandwidth of the four different structures as a function of multiplication gain of 10 μm , 25 μm and 40 μm in diameter.

APD used in optical communication systems generally work in low gain state to obtain better signal-to-noise ratio. As shown in Fig. 3, the superiority of SACMCT is quite obvious compared with the SACM structure in this condition.

For devices of 10 μm in diameter, the high-speed performance is mainly determined by carrier transit time when the multiplication gain is low. Therefore, SACMCT1, which can most effectively reduce the carrier transit time, has the best high-speed performance. The bandwidth of SACMCT1 at unity gain is 33.1 GHz while the bandwidth of SACM at unity gain is 21.6 GHz. It can improve the response speed by 54%. When the gain starts to increase, the high-speed performance of different structures gets closer because the avalanche build up time begins to play an increasingly important role. The gain-bandwidth product of SACM, SACMCT1, SACMCT2

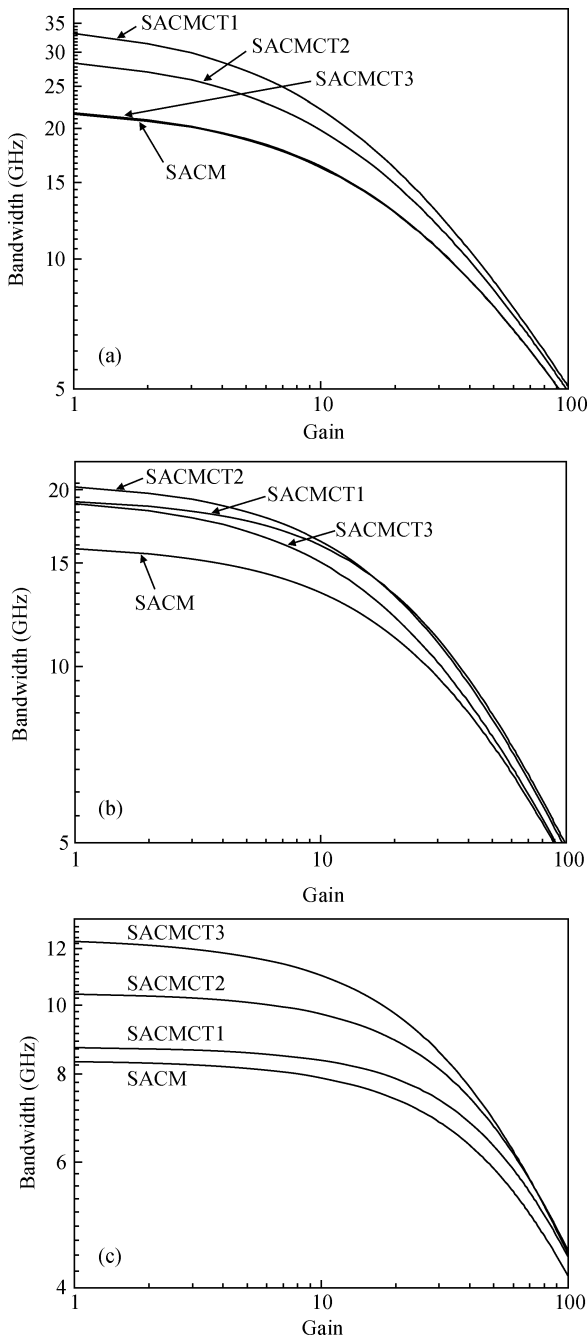


Fig. 3. Gain–bandwidth characteristic of the four different structures of (a) 10 μm in diameter, (b) 25 μm in diameter, and (c) 40 μm in diameter.

and SACMCT3 is 315 GHz, 380 GHz, 356 GHz and 315 GHz respectively.

For devices of 25 μm in diameter, the effect of carrier transit time and capacitance are both important. SACMCT2 which can reduce carrier transit time and capacitance simultaneously has the best high speed performance. The bandwidth of SACMCT2 at unity gain is 20.2 GHz while the bandwidth of SACM at unity gain is 15.8 GHz. It can improve the response speed by 27.4%. SACMCT1 and SACMCT3 are better than the SACM structure too. The gain–bandwidth product of SACM, SACMCT1, SACMCT2 and SACMCT3 is 287 GHz, 334 GHz, 329 GHz and 304 GHz respectively.

For devices of 40 μm in diameter, the high-speed performance is mainly determined by device capacitance. Therefore, SACMCT3, which can reduce the capacitance most effectively, has the best high-speed performance. The bandwidth of SACMCT3 at unity gain is 12.3 GHz while the bandwidth of SACM at unity gain is 8.3 GHz. It can improve the high-speed performance by 47.5%. SACMCT1 and SACMCT2 are also better than SACM. The gain–bandwidth product of SACM, SACMCT1, SACMCT2 and SACMCT3 is 205 GHz, 220 GHz, 244 GHz and 258 GHz respectively.

Devices with different diameters have different capacitance. The proportion of device capacitance–resistance time, carrier transit time, and avalanche build up time is different and the best structure for reducing the most important limiting factor is different. Thus for different device diameters, the SACMCT structure increases the response speed in different levels.

Besides the RCE structure above, the SACMCT structure can be used in undepleted absorber structure^[3], waveguide structure^[5, 6], and large size APD^[4, 10] to reduce their carrier transit time while keeping the capacitance unchanged or even reduced to achieve higher speed.

The calculations above are based on the assumption that electrons inject into the multiplication layer. But it is obvious that SACMCT structure is suitable for the situation of holes injecting into the multiplication layer.

To obtain higher speed, a multiplication layer of 100 nm is reported in Refs. [8, 11], and impact ionization engineering is adopted in Ref. [12]. These can effectively reduce the avalanche build up time. Thus the effect of carrier transit time and capacitance becomes more important and the superiority of SACMCT will become more obvious.

3. Conclusion

In summary, a high-speed avalanche photodiode is proposed in this article. This structure introduces an additional charge layer and transit layer to the separate absorption charge and multiplication structure and therefore could be referred to as separate absorption charge multiplication charge and transit structure. It can improve the 3 dB bandwidth by more than 50% compared with the SACM structure with the same size. The SACMCT APD has great potential to meet the need of optical communication of the future.

References

- [1] Campbell J. Recent advances in telecommunications avalanche photodiodes. *J Lightwave Technol*, 2007, 25(1): 109
- [2] Lenox C, Nie H, Yuan P, et al. Resonant-cavity InGaAs–InAlAs avalanche photodiodes with gain-bandwidth product of 290 GHz. *IEEE Photonics Technol Lett*, 1999, 11(9): 1162
- [3] Li N, Sidhu R, Li X, et al. InGaAs/InAlAs avalanche photodiode with undepleted absorber. *Appl Phys Lett*, 2003, 82(13): 2175
- [4] Shi J W, Wu Z Y, Kuo F M. Planar InAlAs based separated absorption, transport, charge, and multiplication avalanche photodiode with large area and bandwidth-enhancement effect under high-sensitivity operation. 23RD Annual Meeting of the IEEE Photonics Society, 2010: 124
- [5] Kinsey G S, Campbell J C, Dentai A G. Waveguide avalanche photodiode operating at 1.55 μm with a gain–bandwidth product

JOSarXiv.202112.0006V1

- of 320 GHz. IEEE Photonics Technol Lett, 2001, 13(8): 842
- [6] Demiguel S, Zheng X, Li N, et al. Evanescently-coupled avalanche photodiodes integrating a short multimode waveguide for high-responsivity and high-speed applications. Optical Fiber Communication Conference, 2004
- [7] Mai Y, Wang G. Equivalent circuit modeling of separate absorption grading charge multiplication avalanche photodiode. J Light-wave Technol, 2009, 27(9): 1197
- [8] Lahrichi M, Glastre G, Derouin E, et al. 240-GHz gain-bandwidth product back-side illuminated AlInAs avalanche photodiodes. IEEE Photonics Technol Lett, 2010, 22(18): 1373
- [9] Yagyu E, Ishimura E, Nakaji M, et al. Design and characteristics of guardring-free planar AlInAs avalanche photodiodes. J Light-wave Technol, 2009, 27(8): 1011
- [10] Campbell J C, Demiguel S, Ma F, et al. Recent advances in avalanche photodiodes. IEEE J Sel Topics Quantum Electron, 2004, 10(4): 777
- [11] Shimizu S, Shiba K, Nakata T, et al. 40 Gbit/s waveguide avalanche photodiode with p-type absorption layer and thin InAlAs multiplication layer. Electron Lett, 2007, 43(8): 476
- [12] Duan N, Wang S, Ma F, et al. High-speed and low-noise SACM avalanche photodiodes with an impact-ionization-engineered multiplication region. IEEE Photonics Technol Lett, 2005, 17(8): 1719